Synthesis of nanostructures in nanowires using sequential catalyst reactions

F. Panciera[1,2], Y.-C. Chou[2,3,4], M. C. Reuter[2], D. Zakharov[4], E. A. Stach[4], S. Hofmann[1]* and F. M. Ross[2,*]

[1] *Department of Engineering, University of Cambridge, 9 J. J. Thomson Avenue, Cambridge CB3 0FA, UK*

[2] *IBM Research Division, T. J. Watson Research Center, Yorktown Heights, NY 10598, USA*

[3] *Department of Electrophysics, National Chiao Tung University, 1001 University Road, Hsinchu City 300, Taiwan*

[4] *Center for Functional Nanomaterials, Brookhaven National Laboratory, Upton, NY 11973, USA*

* Corresponding authors email: fmross@us.ibm.com, sh315@cam.ac.uk

**Details of Supplementary Movies 1-5**
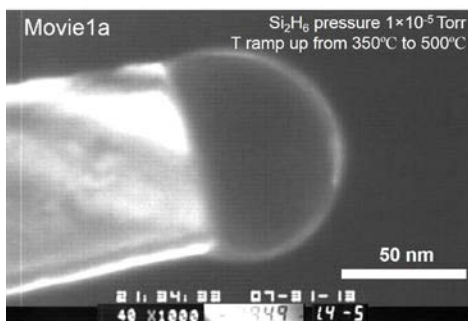
Movie 1: Compilation of sequences that illustrate the formation and incorporation of a $NiSi_2$ nanocrystal in a Si nanowire, recorded using both dark and bright field conditions in the UHV TEM. **a** Formation of silicide nanocrystals on heating a Si nanowire with 1nm Ni from 350 to 500°C in 1×10^{-5} Torr Si_2H_6. **b** Docking of the nanocrystal on the Si(111) interface during exposure to 1×10^{-5} Torr Si_2H_6 at 500°C. Real time. **c** Incorporation of the nanoparticle during heating to 500°C in 1×10^{-5} Torr Si_2H_6. Speeded up 30×.
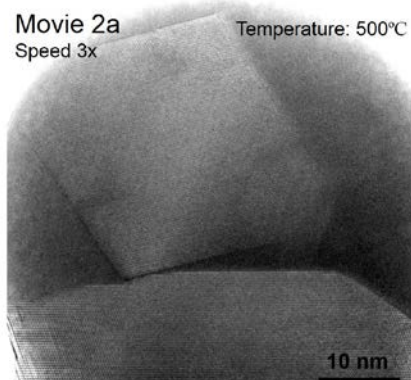

Movie 2: Compilation showing docking of a $NiSi_2$ nanocrystal on the Si(111) interface, recorded at 400 frames per second in the ETEM. **a** Rotation of the nanocrystal after contact; temperature 500°C. Speeded up 3×. **b** Cropped region showing the interface area in **a**, with ledge flow during rotation of the nanocrystal. Slowed down 30×.
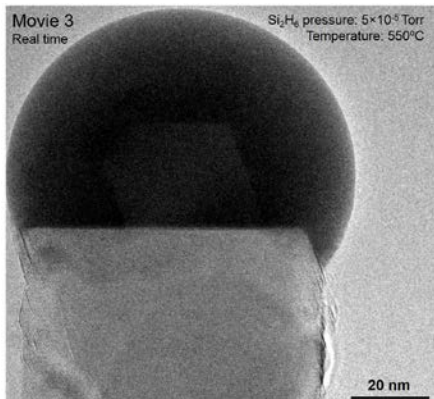
Movie 3: Incorporation of a NiSi$_2$ nanocrystal into a Si nanowire, recorded at 400 frames per second in the ETEM at 550°C in 5×10^{-5} Torr Si$_2$H$_6$. Real time.
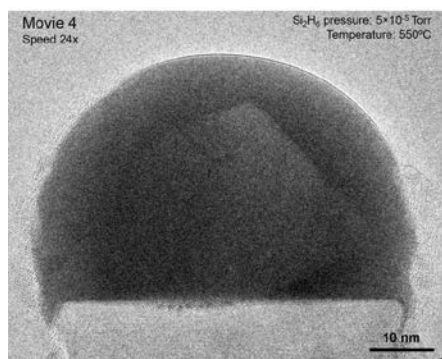
Movie 4: Incorporation of a misoriented NiSi$_2$ nanocrystal into a Si nanowire, recorded at 400 frames per second in the ETEM. at 550°C in 5×10^{-5} Torr Si$_2$H$_6$. Speeded up 30×.
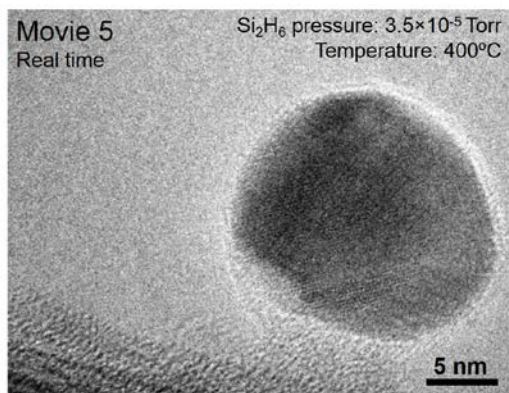

Movie 5: The sequence of phases formed in a 7nm radius polycrystalline Au aerosol particle coated with 0.1 nm of Ni during exposure to 3.5×10^{-5} Torr Si$_2$H$_6$ at 400°C. Real time.

2. The importance of the oxidation step

The method described in Fig. 1 includes an oxidation step where the nanowire is exposed to 10^{-5} Torr O$_2$ before raising the temperature above the eutectic temperature to form and incorporate the NiSi$_2$ nanocrystal. This oxidation step is necessary to prevent metal-silicon reactions at the nanowire surface. Fig. S1 illustrates the result of carrying out the same Ni deposition and anneal but without the presence of O$_2$.

The samples shown had 1nm Ni deposited, then were heated to 360°C (i.e. slightly below the eutectic temperature) in 5×10^{-6} Torr of Si$_2$H$_6$ for 10 min. Under these conditions, the Au$_x$Si$_{1-x}$

catalyst is solid (Fig. S1a). The temperature was then increased by 5°C to induce the transformation of solid Au + Si into liquid Au_xSi_{1-x} eutectic (Fig. S1b). This phase transition happens within 0.1s, consuming part of the nanowire (note the interface receding between Figs. 1a and b). However, immediately afterwards, the droplet size decreased and Au became visible on the sidewalls (Fig. 1c), suggesting surface migration of Au. This is not a coarsening process but a simultaneous collapse of all droplets. (Au migration out of the droplets could in principle be driven by coarsening [1], but at this temperature the process would be slow.) The final equilibrium shape of the droplet (Fig. 1d) exhibits a small wetting angle (~30°) and volume reduced by ~6×. Inside the remaining Au_xSi_{1-x} liquid, nanocrystals with bright contrast (arrows in Fig. 1d) are visible; these were identified as Ni silicides.
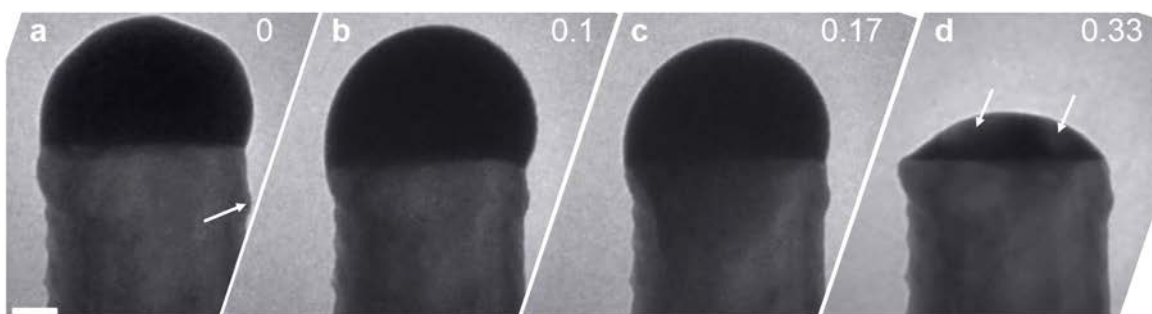

Figure S1: Sequence of bright field TEM images recorded during annealing at 370°C and 5×10^{-6} Torr Si_2H_6. The Si nanowire is covered by 1 nm of Ni deposited by e-beam evaporation. The time is shown in seconds since the first image. The scale bar is 20 nm. The arrowed feature in **a** is used as reference to align the images. **a** the wires were held for 10 min a few degrees below the Au-Si eutectic temperature, then at t=0 the temperature was increased by 10°C. **b** A rapid reaction forms liquid Au_xSi_{1-x}. **c** Rapidly the Au_xSi_{1-x} droplet shrinks and Au becomes visible at the nanowire surface as a dark shadow; **d** Au has mostly diffused away from the droplet. Two silicide nanocrystals (bright contrast) are visible inside the remaining liquid.

We believe that the migration of Au from the droplet is induced by a change in the nanowire sidewall energy that modifies the equilibrium droplet shape. It is well known that the deposition of a few nm of Ni on clean Si by evaporation [2] or sputtering [3] induces the formation of a Ni-Si amorphous intermixed layer, even at room temperature. This layer, after successive annealing steps, crystallizes into a nickel silicide phase: sub-nanometer layers deposited by e-beam evaporation and annealed 450-550°C result in $NiSi_2$, while sputtered layers usually form the metastable θ-Ni_2Si. Under our deposition and annealing conditions we therefore expect to form a thin $NiSi_2$ layer on the nanowire sidewalls. Such a layer would have a surface energy higher than silicon [4,5] and could therefore be responsible for destabilizing the droplets by inducing Au migration. The oxidation step, carried out at 200°C in 1×10^{-5} Torr of O_2 for 30 min, results in a SiO_2 layer at the nanowire surface through the following mechanism: first Ni

reacts with Si forming one of the silicide phases; second, the silicide decomposes into Ni + SiO_2 since the reaction of Si with oxygen to form SiO_2 is energetically favorable with respect to NiO; finally the resulting nickel migrates though the silicide layer and reacts at the silicon-silicide interface to form more silicide [6]. On the Au_xSi_{1-x} droplet, the Ni rapidly forms an alloy with Au and reacts with oxygen. However at this temperature the reaction is slow and the complete consumption of Ni requires several days [7].

3. Incorporation of multiple silicides
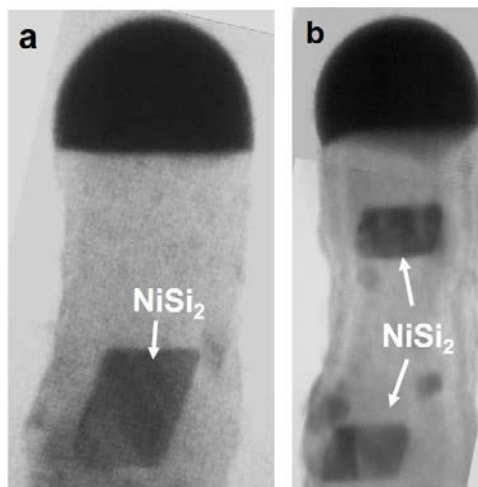
Figure S2: Bright field TEM images showing silicides incorporated into Si nanowires. **a** Single silicide incorporated during growth at 500°C and 5×10^{-6} Torr Si_2H_6. **b** Same sample in **a** but a different wire after repeating the process of formation and incorporation of silicide nanoparticles.

4. Determination of the Ni-silicide phases

First phase

Growth experiments such as those in Fig. 3b and 3c do not identify the first silicide phase directly because of the relatively low spatial resolution. Instead, we infer the silicide phase from two clues: the time to nucleation of Si, and the volume changes of the silicide.

(a) First consider the timing of the phases in Fig. 3b and 3c. As was done in Ref. 26, the rate at which Au shrinks can be used to determine the arrival rate of Si atoms into the Au particle. The complete reaction of Au and Si to form Au_xSi_{1-x} happens after 2400s at t=3010s, and the Au reacts at a rate of 0.9 nm^3/s. This corresponds to a rate of Si introduction into the droplet of 33 atoms per sec (i.e. 0.13 nm^3/s). We assume that Si continues to arrive at this rate throughout the remainder of the experiment (i.e. that the sticking probability is constant). After the Si particle nucleates, its growth rate is 0.16 nm^3/s, consistent with this assumption.

Given this arrival rate for Si, we now calculate the expected time at which Si should nucleate, in the absence of any Ni reactions, based on the compositions at the liquidus lines at the

growth temperature [8]. Si nucleation would be expected at t=4070s but was actually observed at t=6400s. Clearly not all of the incoming Si was used to increase the Si content in the Au_xSi_{1-x}. Instead, the additional ~2330s corresponds to ~2400 nm^3 Si (129000 atoms) and these transform the Ni-rich phase to $NiSi_2$. The final $NiSi_2$ volume of ~1800 nm^3 contained ~182000 atoms of Si, so the initial phase contained 182000-129000=53000 atoms. The ratio is 3.4, consistent with the ratio 4 expected for the transformation from Ni_2Si to $NiSi_2$.

(b) Another clue comes from the change in volume between the initial Ni-rich phase and the final $NiSi_2$ phase. In Fig. 3b and 3c, the silicide forms and remains at a constant volume for the first 2500 s then its volume changes by a factor ~2.2 after the complete consumption of solid Au. This is consistent with an initial phase of Ni_2Si, which in Table S1 is expected to show a volume ratio of 2.37 with $NiSi_2$.

Last phase

Two pieces of evidence suggest that the octahedral nanocrystal is the Si-rich silicide phase $NiSi_2$. First, the octahedral shape composed of {111} facets is consistent with the lowest energy configuration for a crystallite of cubic structure. Second, the lattice parameter and epitaxy with Si are consistent with $NiSi_2$, as it is the only nickel silicide that is cubic and has a lattice parameter close to Si (0.4% mismatch).

The formation of $NiSi_2$ at low temperature appears in disagreement with what is generally observed during the solid state reaction of Ni and Si thin films and the respective bulk diffusion couples [9,10]. Both the free energy gain (ΔG) and surface energy gain of silicide formation are presumably altered in the presence of Au. Unfortunately neither the ternary Au-Ni-Si phase diagram nor data about silicide/Au_xSi_{1-x} interface energies are available. However, alloying Au with Ni is known to favor nucleation and growth of Ni silicides at low temperature [11]. The same has been found for Co [12]. Thus, the presence of the catalyst may allow lower temperature formation of phases than would be possible otherwise. Moreover, the solubility of Au is known to be about 20 times higher in $NiSi_2$ than in the commonly observed Ni-rich phase, Ni_2Si, at 300°C [13]. The presence of Au may thus favor formation of $NiSi_2$ by increasing its ΔG with respect to the other phases, due to the increase in the total entropy of mixing of the system.
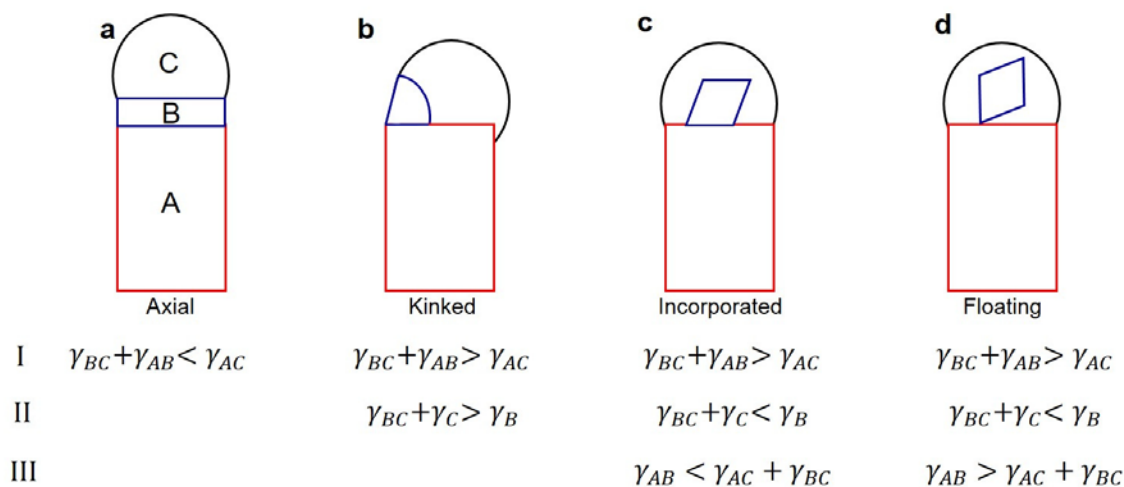
5. Silicide nucleation before Au-Si reaction

If we hold nanowires similar to those in Fig. 1 below the eutectic temperature, we can observe the phase sequence directly without rapid formation of Au_xSi_{1-x} liquid. In Fig. S3 below, the Au remains solid. A silicide forms before the Au has reacted to form Au_xSi_{1-x}, the same sequence that took place in Fig. 3.
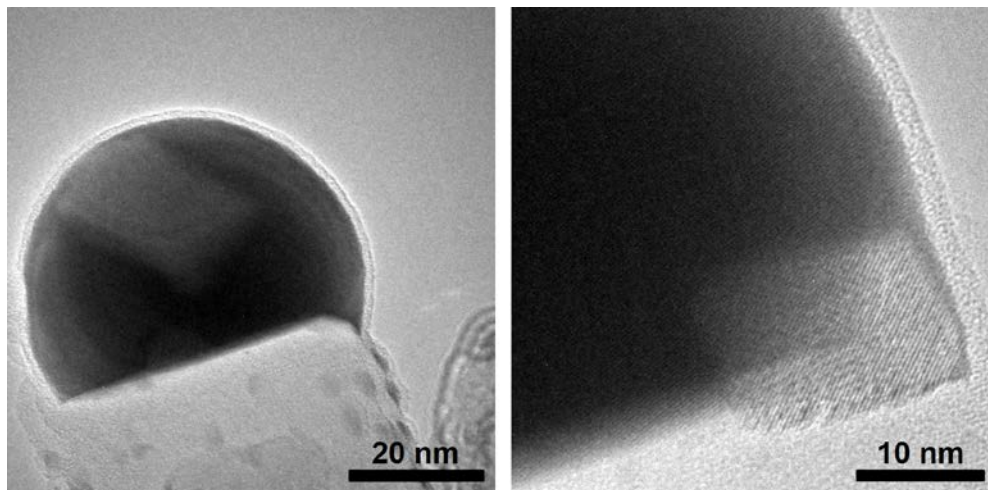
Figure S3: TEM images of Ni-silicides forming in a solid Au catalyst at the tip of a Si nanowire. The nanowires were coated with ~1nm of Ni and annealed for one hour at 300C. Ni-silicide forms while the Au remains solid. Formation at two different locations is shown, at the interface and at the droplet surface.

6. Thermodynamic constraints for endotaxial crystal formation

A necessary condition for the formation of straight (as opposed to kinked) nanowire heterojunctions was developed in Ref. [14]. Fig. S4 extends this simple model further to address the necessary conditions for creation of nanowires containing endotaxial inclusions. The first requirement is that the system should form a compact nanocrystal instead of a full layer of the new material. This requires a specific relationship between the interface energies of the various crystals, shown in line I. However, for endotaxy the newly formed, compact crystal should be completely wetted by the liquid catalyst otherwise it will form at the nanowire surface. This leads to the inequality in line II. Finally, the attachment and subsequent incorporation of the new crystal requires the inequality relating the interface energy between the two crystals in line III.

I	$\gamma_{BC} + \gamma_{AB} < \gamma_{AC}$	$\gamma_{BC} + \gamma_{AB} > \gamma_{AC}$	$\gamma_{BC} + \gamma_{AB} > \gamma_{AC}$	$\gamma_{BC} + \gamma_{AB} > \gamma_{AC}$
II		$\gamma_{BC} + \gamma_C > \gamma_B$	$\gamma_{BC} + \gamma_C < \gamma_B$	$\gamma_{BC} + \gamma_C < \gamma_B$
III			$\gamma_{AB} < \gamma_{AC} + \gamma_{BC}$	$\gamma_{AB} > \gamma_{AC} + \gamma_{BC}$

Figure S4: Schematic representing four kinds of heterostructures obtainable as a function of three conditions for the surface energies of the nanowire, droplet and nanocrystal. γ_{AB} is the interface energy between A and B, while γ_A is the surface energy of A, with other terms defined analogously. **a** represents the case of axial heterostrucures; **b** the case that induces the wire kinking (both adapted from Ref. [14]); **c** is the case of the incorporation of a compact nanocrystal and **d** the nanocrystal floating in the liquid.

Phase	Structure/ Group	Lattice			Silicide V per Ni atom (Å^3)	NiSi$_2$/Silicide V (Å^3)
		a (Å)	b (Å)	c(Å)		
Ni	Cubic/Fm3m	3.5238			10.94	3.61
Ni$_3$Si	Cubic/Pm3m	3.5056			14.36	2.75
Ni$_{31}$Si$_{12}$	Hex/p3$_2$1	6.671		12.288	15.28	2.58
δ-Ni$_2$Si	Orthor/Pnma	4.99	3.72	7.06	16.07	2.37
θ-Ni$_2$Si	Hex/P6$_3$/mmc	3.80		4.89		
Ni$_3$Si$_2$	Orthor/Cmc21	12.29	10.805	6.924	19.16	2.06
NiSi	Orthor/Pnma	5.233	3.258	5.659	24.12	1.64
α-NiSi$_2$	Cubic/Fm3m	5.416			39.5	1
Si	Cubic/Fd3m	5.4309				

Table S1: Structure of nickel silicide phases [10]

References

[1] Hannon, J. B., Kodambaka, S., Ross F. M., Tromp, R. M. The influence of the surface migration of gold on the growth of silicon nanowires. *Nature* **440**, 69-71 (2006).

[2] Tung, R. T., Gibson, J. M., Poate, J. M. Formation of ultrathin single-crystal silicide films on Si: Surface and interfacial stabilization of Si-NiSi$_2$ epitaxial structures. *Phys. Rev. Lett*. **50**, 429-432 (1983).

[3] De Keyser, K. Phase formation and thermal stability of ultrathin nickel-silicides on Si(100). *Appl. Phys. Lett.* **96**, 173503 (2010).

[4] Vasiliu M. I., Eremenko, V. N. The surface tension of liquid nickel-silicon alloys. *Poroshkovaya Metallurgica* **3**(27), 80-82 (1965).

[5] Lee, P. S., Pey, K. L., Mangelinck, D., Chi D. Z., Osipowicz, T. On the morphological changes of Ni- and Ni(Pt)-Silicides. *J. Electrochem. Soc.* **152**, G305-G308 (2005).

[6] Bartur, M., Nicolet, M. A. Thermal oxidation of nickel disilicide. *Appl. Phys. Lett.* **40**, 175 (1982).

[7] Khan H., Francombe, M. H., Structure and oxidation of thin gold-nickel alloy films. *J. Appl. Phys.* **36**, 1699 (1965).

[8] Kim, B J. et al. Kinetics of individual nucleation events observed in nanoscale vapor-liquid-solid growth. Science **322**, 1070 (2008).

[9] Lavoie, C., d'Heurle, F.M., Detavernier, C., Cabral, C. Jr. Towards implementation of a nickel silicide process for CMOS technologies. Microelecron. Eng. **70,** 144–157 (2003).

[10] Lavoie, C., Detavernier, C., Besser, P. Silicide Technology for Integrated Circuits, p. 102, *The Institution of Engineering and Technology*, London, UK (2009).

[11] Hung, L. S., Zheng, L. R., Mayer, J. W., Influence of Au as an impurity in Ni-silicide growth. *J. Appl. Phys.* **54**, 792 (1983).

[12] Detavernier, C., Lavoie, C., d'Heurle, F. M., Bender H., Van Meirhaeghe, R. L. Low-temperature formation of CoSi$_2$ in the presence of Au. *J. Appl. Phys.* **95**, 5340 (2004).

[13] Mangelinck, D., Gas, P., Grob, A., Pichaud, B., Thomas, O. Formation of Ni silicide from Ni (Au) films on (111) Si. *J. Appl. Phys.* **79**, 4078−4086 (1996).

[14] Dick, K. A. *et al.* The morphology of axial and branched nanowire heterostructures. *Nano Letters* **7**, 1817-1822 (2007).